

# Electronic Schrödinger equation with nonclassical nuclei

Yasumitsu Suzuki,<sup>1</sup> Ali Abedi,<sup>1</sup> Neepa T. Maitra,<sup>2</sup> Koichi Yamashita,<sup>3</sup> and E. K. U. Gross<sup>1</sup>

<sup>1</sup>Max-Planck-Institut für Mikrostrukturphysik, Weinberg 2, D-06120 Halle, Germany

<sup>2</sup>Department of Physics and Astronomy, Hunter College and the City University of New York, 695 Park Avenue, New York, New York 10065, USA

<sup>3</sup>Department of Chemical System Engineering, School of Engineering, The University of Tokyo, 7-3-1 Hongo, Bunkyo-ku, Tokyo 113-8656, Japan

(Received 13 November 2013; published 21 April 2014)

We present a rigorous reformulation of the quantum mechanical equations of motion for the coupled system of electrons and nuclei that focuses on the dynamics of the electronic subsystem. Usually the description of electron dynamics involves an electronic Schrödinger equation where the nuclear degrees of freedom appear as parameters or as classical trajectories. Here we derive the exact Schrödinger equation for the subsystem of electrons, staying within a full quantum treatment of the nuclei. This exact Schrödinger equation features a time-dependent potential energy surface for electrons (*e*-TD PES). We demonstrate that this exact *e*-TD PES differs significantly from the electrostatic potential produced by classical or quantum nuclei.

DOI: 10.1103/PhysRevA.89.040501

PACS number(s): 31.50.-x, 31.15.-p, 82.20.Gk

The theoretical description of electronic motion in the time domain is among the biggest challenges in theoretical physics. A variety of tools has been developed to tackle this problem, among them the Kadanoff-Baym approach [1], time-dependent density functional theory [2], the hierarchical equations of motion approach [3], and the multiconfiguration time-dependent Hartree-Fock approach [4]. From the point of view of electronic dynamics all these approaches are formally exact as long as the nuclei are considered clamped. However, some of the most fascinating phenomena result from the coupling of electronic and nuclear motion, e.g., photovoltaics [5], processes in vision [6], photosynthesis [7], molecular electronics [8], and strong-field processes [9]. To properly capture electron dynamics in these phenomena, it is essential to account for electron-nuclear (*e*-*n*) coupling.

In principle, the *e*-*n* dynamics is described by the complete time-dependent Schrödinger equation (TDSE)

$$\hat{H}\Psi(\underline{\mathbf{r}},\underline{\mathbf{R}},t) = i\partial_t\Psi(\underline{\mathbf{r}},\underline{\mathbf{R}},t), \quad (1)$$

with Hamiltonian

$$\hat{H} = \hat{T}_n(\underline{\mathbf{R}}) + \hat{V}_{\text{ext}}^n(\underline{\mathbf{R}},t) + \hat{H}_{\text{BO}}(\underline{\mathbf{r}},\underline{\mathbf{R}}) + \hat{v}_{\text{ext}}^e(\underline{\mathbf{r}},t), \quad (2)$$

where  $\hat{H}_{\text{BO}}(\underline{\mathbf{r}},\underline{\mathbf{R}})$  is the traditional Born-Oppenheimer (BO) electronic Hamiltonian,

$$\hat{H}_{\text{BO}} = \hat{T}_e(\underline{\mathbf{r}}) + \hat{W}_{ee}(\underline{\mathbf{r}}) + \hat{W}_{en}(\underline{\mathbf{r}},\underline{\mathbf{R}}) + \hat{W}_{nn}(\underline{\mathbf{R}}). \quad (3)$$

Here  $\hat{T}_n = -\sum_{\alpha=1}^{N_n} \frac{\nabla_{\alpha}^2}{2M_{\alpha}}$  and  $\hat{T}_e = -\sum_{j=1}^{N_e} \frac{\nabla_j^2}{2m}$  are the nuclear and electronic kinetic energy operators,  $\hat{W}_{ee}$ ,  $\hat{W}_{en}$ , and  $\hat{W}_{nn}$  are the electron-electron, *e*-*n*, and nuclear-nuclear interaction, and  $\hat{V}_{\text{ext}}^n(\underline{\mathbf{R}},t)$  and  $\hat{v}_{\text{ext}}^e(\underline{\mathbf{r}},t)$  are time-dependent (TD) external potentials acting on the nuclei and electrons, respectively. Throughout this paper  $\underline{\mathbf{R}}$  and  $\underline{\mathbf{r}}$  collectively represent the nuclear and electronic coordinates, respectively, and  $\hbar = 1$ .

A full numerical solution of the complete *e*-*n* TDSE, Eq. (1), is extremely hard to achieve and has been obtained only for small systems with very few degrees of freedom, such as  $\text{H}_2^+$  [10]. For larger systems, an efficient and widely used approximation is the mixed quantum-classical description

where the electrons are propagated quantum mechanically according to the TDSE

$$[\hat{T}_e(\underline{\mathbf{r}}) + \hat{W}_{ee}(\underline{\mathbf{r}}) + V(\underline{\mathbf{r}},t) + \hat{v}_{\text{ext}}^e(\underline{\mathbf{r}},t)]\Phi(\underline{\mathbf{r}},t) = i\partial_t\Phi(\underline{\mathbf{r}},t), \quad (4)$$

which is coupled to the classical nuclear trajectories  $\underline{\mathbf{R}}_{\alpha}(t)$ , determined by Ehrenfest or surface-hopping algorithms [11]. The potential  $V(\underline{\mathbf{r}},t)$  experienced by the electrons is then given by the classical expression

$$V_{\text{class}}(\underline{\mathbf{r}},t) = W_{en}(\underline{\mathbf{r}},\underline{\mathbf{R}}(t)) = -\sum_{j=1}^{N_e} \sum_{\alpha=1}^{N_n} \frac{eZ_{\alpha}}{|\mathbf{r}_j - \mathbf{R}_{\alpha}(t)|}, \quad (5)$$

where  $\underline{\mathbf{R}}(t)$  denotes the set of classical nuclear trajectories  $\underline{\mathbf{R}}_{\alpha}(t)$ . A better approximation to the potential  $V(\underline{\mathbf{r}},t)$  experienced by the electrons is the electrostatic or Hartree expression [11]:

$$V_{\text{Hartree}}(\underline{\mathbf{r}},t) = -eZ_{\alpha} \sum_{j=1}^{N_e} \sum_{\alpha=1}^{N_n} \int d\underline{\mathbf{R}} \frac{|\chi(\underline{\mathbf{R}},t)|^2}{|\mathbf{r}_j - \mathbf{R}_{\alpha}|}, \quad (6)$$

where  $\chi(\underline{\mathbf{R}},t)$  represents a nuclear many-body wave function obtained, e.g., from nuclear wave packet dynamics. Clearly, Eq. (6) reduces to the classical expression (5) in the limit of very narrow wave packets centered around the classical trajectories  $\underline{\mathbf{R}}(t)$ . The Hartree expression (6) incorporates the nuclear charge distribution, but the potential is still approximate as it neglects *e*-*n* correlations.

In this paper we address the question of whether the potential  $V(\underline{\mathbf{r}},t)$  in the purely electronic many-body TDSE, Eq. (4), can be chosen such that the resulting electronic wave function  $\Phi(\underline{\mathbf{r}},t)$  becomes *exact*. By exact we mean that  $\Phi(\underline{\mathbf{r}},t)$  reproduces the true electronic  $N_e$ -body density and the true  $N_e$ -body current density that would be obtained from the full *e*-*n* wave function  $\Psi(\underline{\mathbf{r}},\underline{\mathbf{R}},t)$  of Eq. (1). We shall demonstrate that the answer is yes, provided we allow for a vector potential  $\mathbf{S}(\underline{\mathbf{r}},t)$  in the electronic TDSE, in addition to the scalar potential  $\bar{V}(\underline{\mathbf{r}},t)$ . We will analyze this potential for an exciting experiment, namely, the laser-induced localization

of the electron in the  $H_2^+$  molecule [12]. We find significant differences between this exact potential and both the classical-nuclei potential Eq. (5) and the Hartree potential Eq. (6).

References [13,14] proved that the *exact* solution of the complete molecular TDSE Eq. (1) can be written as a single product

$$\Psi(\underline{\mathbf{r}}, \underline{\mathbf{R}}, t) = \Phi(\underline{\mathbf{r}}, t) \chi(\underline{\mathbf{R}}, t) \quad (7)$$

of a nuclear wave function  $\chi(\underline{\mathbf{R}}, t)$ , and an electronic wave function parametrized by the nuclear coordinates  $\Phi(\underline{\mathbf{r}}, t)$ , which satisfies the partial normalization condition (PNC)  $\int d\underline{\mathbf{r}} |\Phi(\underline{\mathbf{r}}, t)|^2 = 1$ . Here we instead consider the *reverse* factorization,

$$\Psi(\underline{\mathbf{r}}, \underline{\mathbf{R}}, t) = \chi(\underline{\mathbf{R}}, t) \Phi(\underline{\mathbf{r}}, t). \quad (8)$$

It is straightforward to see that the formalism presented in Ref. [13] follows through simply with a switch of the role of electronic and nuclear coordinates. In particular, we have the following:

(i) The exact solution of the TDSE may be written as Eq. (8), where  $\chi(\underline{\mathbf{R}}, t)$  satisfies the PNC  $\int d\underline{\mathbf{R}} |\chi(\underline{\mathbf{R}}, t)|^2 = 1$ .

(ii) The nuclear wave function  $\chi(\underline{\mathbf{R}}, t)$  satisfies

$$[\hat{H}_n(\underline{\mathbf{R}}, \underline{\mathbf{r}}, t) - \epsilon_e(\underline{\mathbf{r}}, t)] \chi(\underline{\mathbf{R}}, t) = i \partial_t \chi(\underline{\mathbf{R}}, t), \quad (9)$$

with the nuclear Hamiltonian

$$\begin{aligned} \hat{H}_n(\underline{\mathbf{R}}, \underline{\mathbf{r}}, t) = & \hat{T}_n(\underline{\mathbf{R}}) + \hat{W}_{ee}(\underline{\mathbf{r}}) + \hat{W}_{en}(\underline{\mathbf{r}}, \underline{\mathbf{R}}) + \hat{W}_{nn}(\underline{\mathbf{R}}) \\ & + \hat{v}_{\text{ext}}^e(\underline{\mathbf{r}}, t) + \hat{V}_{\text{ext}}^n(\underline{\mathbf{R}}, t) \\ & + \sum_{j=1}^{N_e} \frac{1}{m} \left[ \frac{[-i\nabla_j - \mathbf{S}_j(\underline{\mathbf{r}}, t)]^2}{2} \right. \\ & \left. + \left( \frac{-i\nabla_j \Phi}{\Phi} + \mathbf{S}_j(\underline{\mathbf{r}}, t) \right) [-i\nabla_j - \mathbf{S}_j(\underline{\mathbf{r}}, t)] \right]. \end{aligned} \quad (10)$$

The electronic wave function  $\Phi(\underline{\mathbf{r}}, t)$  satisfies the TDSE

$$\left( \sum_{j=1}^{N_e} \frac{1}{2m} [-i\nabla_j + \mathbf{S}_j(\underline{\mathbf{r}}, t)]^2 + \epsilon_e(\underline{\mathbf{r}}, t) \right) \Phi(\underline{\mathbf{r}}, t) = i \partial_t \Phi(\underline{\mathbf{r}}, t). \quad (11)$$

Here the exact TD potential energy surface for electrons (*e*-TDPES)  $\epsilon_e(\underline{\mathbf{r}}, t)$  and the exact electronic TD vector potential  $\mathbf{S}_j(\underline{\mathbf{r}}, t)$  are defined as

$$\epsilon_e(\underline{\mathbf{r}}, t) = \langle \chi(\underline{\mathbf{R}}, t) | \hat{H}_n(\underline{\mathbf{R}}, \underline{\mathbf{r}}, t) - i \partial_t | \chi(\underline{\mathbf{R}}, t) \rangle_{\underline{\mathbf{R}}}, \quad (12)$$

$$\mathbf{S}_j(\underline{\mathbf{r}}, t) = \langle \chi(\underline{\mathbf{R}}, t) | -i \nabla_j | \chi(\underline{\mathbf{R}}, t) \rangle_{\underline{\mathbf{R}}}, \quad (13)$$

where  $\langle \dots | \dots \rangle_{\underline{\mathbf{R}}}$  denotes a matrix element integrating over all nuclear variables only.

(iii) Equations (9)–(11) are form invariant under the gaugelike transformation  $\chi(\underline{\mathbf{R}}, t) \rightarrow \tilde{\chi}(\underline{\mathbf{R}}, t) = \exp[i\theta(\underline{\mathbf{r}}, t)] \chi(\underline{\mathbf{R}}, t)$ ,  $\Phi(\underline{\mathbf{r}}, t) \rightarrow \tilde{\Phi}(\underline{\mathbf{r}}, t) = \exp[-i\theta(\underline{\mathbf{r}}, t)] \Phi(\underline{\mathbf{r}}, t)$ , while the potentials transform as  $\mathbf{S}_j(\underline{\mathbf{r}}, t) \rightarrow \tilde{\mathbf{S}}_j(\underline{\mathbf{r}}, t) = \mathbf{S}_j(\underline{\mathbf{r}}, t) + \nabla_j \theta(\underline{\mathbf{r}}, t)$ ,  $\epsilon_e(\underline{\mathbf{r}}, t) \rightarrow \tilde{\epsilon}_e(\underline{\mathbf{r}}, t) = \epsilon_e(\underline{\mathbf{r}}, t) + \partial_t \theta(\underline{\mathbf{r}}, t)$ . The wave functions  $\chi(\underline{\mathbf{R}}, t)$  and  $\Phi(\underline{\mathbf{r}}, t)$

yielding a given solution  $\Psi(\underline{\mathbf{r}}, \underline{\mathbf{R}}, t)$  of Eq. (1) are unique up to this  $(\underline{\mathbf{r}}, t)$ -dependent phase transformation.

(iv) The wave functions  $\chi(\underline{\mathbf{R}}, t)$  and  $\Phi(\underline{\mathbf{r}}, t)$  are interpreted as nuclear and electronic wave functions:  $|\Phi(\underline{\mathbf{r}}, t)|^2 = \int |\Psi(\underline{\mathbf{r}}, \underline{\mathbf{R}}, t)|^2 d\underline{\mathbf{R}}$  is the probability density of finding the electronic configuration  $\underline{\mathbf{r}}$  at time  $t$ , and  $|\chi(\underline{\mathbf{R}}, t)|^2 = |\Psi(\underline{\mathbf{r}}, \underline{\mathbf{R}}, t)|^2 / |\Phi(\underline{\mathbf{r}}, t)|^2$  is the conditional probability of finding the nuclei at  $\underline{\mathbf{R}}$ , given that the electronic configuration is  $\underline{\mathbf{r}}$ . The exact electronic  $N_e$ -body current density can be obtained from  $\text{Im}(\Phi^* \nabla_j \Phi) + |\Phi(\underline{\mathbf{r}}, t)|^2 \mathbf{S}_j$ .

We can regard Eq. (11) as the *exact electronic TDSE*: The time evolution of  $\Phi(\underline{\mathbf{r}}, t)$  is completely determined by the exact *e*-TDPES  $\epsilon_e(\underline{\mathbf{r}}, t)$  and the vector potential  $\mathbf{S}_j(\underline{\mathbf{r}}, t)$ . Moreover, these potentials are *unique* up to within a gauge transformation (iii, above). In other words, if one requires a purely electronic TDSE (11) with solution  $\Phi(\underline{\mathbf{r}}, t)$  to yield the true electron ( $N_e$ -body) density and current density of the full *e-n* problem, then the potentials appearing in this TDSE are (up to within a gauge transformation) uniquely given by Eqs. (12) and (13).

A formalism in which the nuclear wave function is conditionally dependent on the electronic coordinates, rather than the other way around, may appear somewhat nonintuitive. However, in many nonadiabatic processes, the nuclear and electronic speeds are comparable, and, in some cases, such as highly excited Rydberg molecules, nuclei may even move faster than electrons [15]. We shall show in the following that the present factorization is useful for interpreting the dynamics of attosecond electron localization, and that it gives direct insight into how the *e-n* coupling affects nonadiabatic electron dynamics. For this purpose it is useful to rewrite the exact *e*-TDPES as

$$\epsilon_e(\underline{\mathbf{r}}, t) = \epsilon_e^{\text{approx}}(\underline{\mathbf{r}}, t) + \Delta\epsilon_e(\underline{\mathbf{r}}, t), \quad (14)$$

where

$$\begin{aligned} \epsilon_e^{\text{approx}}(\underline{\mathbf{r}}, t) = & \langle \chi(\underline{\mathbf{R}}, t) | \hat{W}_{ee}(\underline{\mathbf{r}}) + \hat{W}_{en}(\underline{\mathbf{r}}, \underline{\mathbf{R}}) + \hat{W}_{nn}(\underline{\mathbf{R}}) \\ & + \hat{v}_{\text{ext}}^e(\underline{\mathbf{r}}, t) + \hat{V}_{\text{ext}}^n(\underline{\mathbf{R}}, t) | \chi(\underline{\mathbf{R}}, t) \rangle_{\underline{\mathbf{R}}} \end{aligned} \quad (15)$$

and

$$\begin{aligned} \Delta\epsilon_e(\underline{\mathbf{r}}, t) = & \langle \chi(\underline{\mathbf{R}}, t) | \hat{T}_n(\underline{\mathbf{R}}) | \chi(\underline{\mathbf{R}}, t) \rangle_{\underline{\mathbf{R}}} + \langle \chi(\underline{\mathbf{R}}, t) | -i \partial_t | \chi(\underline{\mathbf{R}}, t) \rangle_{\underline{\mathbf{R}}} \\ & + \sum_{j=1}^{N_e} \frac{\langle \nabla_j \chi(\underline{\mathbf{R}}, t) | \nabla_j \chi(\underline{\mathbf{R}}, t) \rangle_{\underline{\mathbf{R}}}}{2m} - \sum_{j=1}^{N_e} \frac{\mathbf{S}_j^2(\underline{\mathbf{r}}, t)}{2m}. \end{aligned} \quad (16)$$

If the nuclear density is approximated as a  $\delta$  function at  $\underline{\mathbf{R}}(t)$ , then  $\epsilon_e^{\text{approx}}$  reduces to the electronic potential used in the traditional mixed quantum-classical approximations:

$$\begin{aligned} \epsilon_e^{\text{trad}}(\underline{\mathbf{r}}, t) = & \hat{W}_{ee}(\underline{\mathbf{r}}) + \hat{W}_{en}(\underline{\mathbf{r}}, \underline{\mathbf{R}}(t)) + \hat{W}_{nn}(\underline{\mathbf{R}}(t)) \\ & + \hat{v}_{\text{ext}}^e(\underline{\mathbf{r}}, t) + \hat{V}_{\text{ext}}^n(\underline{\mathbf{R}}(t)). \end{aligned} \quad (17)$$

This approximation not only neglects the width of the nuclear wavefunction but also misses the contribution to the potential from  $\Delta\epsilon_e(\underline{\mathbf{r}}, t)$ , Eq. (16). Methods that retain a quantum description of the nuclei (e.g., the TD Hartree approach [11]) approximate Eq. (15), although without the parametric dependence of the nuclear wave function on  $\underline{\mathbf{r}}$ , and still miss the contribution from Eq. (16). In the following

example, we will show the significance of the  $e$ - $n$  correlation represented in the term  $\Delta\epsilon_e$ .

Among the many charge-transfer processes accompanying nuclear motion mentioned earlier, here we study attosecond electron localization dynamics in the dissociation of the  $\text{H}_2^+$  molecule achieved by time-delayed coherent ultrashort laser pulses [12]. In the experiment, first an ultraviolet (UV) pulse excites  $\text{H}_2$  to the dissociative  $2p\sigma_u$  state of  $\text{H}_2^+$  while a second time-delayed infrared (IR) pulse induces electron transfer between the dissociating atoms. This relatively recent technique has gathered increasing attention since it is expected to eventually lead to the direct control of chemical reactions via the control of electron dynamics. Extensive theoretical studies have led to progress in understanding the mechanism [12], and highlight the important role of  $e$ - $n$  correlated motion. Here we study the exact  $e$ - $n$  coupling terms by computing the exact  $e$ -TD PES Eq. (12).

We consider a one-dimensional  $\text{H}_2^+$  model, starting the dynamics after the excitation by the UV pulse: the wave packet starts at  $t=0$  on the first excited state ( $2p\sigma_u$  state) of  $\text{H}_2^+$  as a Frank-Condon projection of the wave function of the ground state, and then is exposed to the IR laser pulse. The Hamiltonian is given by Eq. (2), with  $\mathbf{R} \rightarrow R$ , the internuclear distance, and  $\mathbf{r} \rightarrow z$ , the electronic coordinate as measured from the nuclear center of mass [16]. The kinetic energy terms are  $\hat{T}_n(R) = -\frac{1}{2\mu_n} \frac{\partial^2}{\partial R^2}$  and  $\hat{T}_e(z) = -\frac{1}{2\mu_e} \frac{\partial^2}{\partial z^2}$ , respectively, where the reduced mass of the nuclei is given by  $\mu_n = M_H/2$ , and the reduced electronic mass is given by  $\mu_e = \frac{2M_H}{2M_H+1}$  ( $M_H$  is the proton mass). The interactions are soft Coulomb:  $\hat{W}_{nn}(R) = \frac{1}{\sqrt{0.03+R^2}}$ , and  $\hat{W}_{en}(z, R) = -\frac{1}{\sqrt{1.0+(z-R/2)^2}} - \frac{1}{\sqrt{1.0+(z+R/2)^2}}$  (and  $\hat{W}_{ee} = 0$ ). The IR pulse is taken into account using the dipole approximation and length gauge, as  $\hat{v}_{\text{ext}}^e(z, t) = E(t)q_e z$ , where  $E(t) = E_0 \exp[-(\frac{t-\Delta t}{\tau})^2] \cos[\omega(t - \Delta t)]$ , and the reduced charge  $q_e = \frac{2M_H+2}{2M_H+1}$ . The wavelength is 800 nm and the peak intensity  $I_0 = E_0^2 = 3.0 \times 10^{12} \text{ W/cm}^2$ . The pulse duration is  $\tau = 4.8 \text{ fs}$  and  $\Delta t$  is the time delay between the UV and IR pulses. Here we show the results for  $\Delta t = 7 \text{ fs}$ . We propagate the full TDSE (1) numerically exactly to obtain the full molecular wave function  $\Psi(z, R, t)$ , and from it we calculate the probabilities of directional localization of the electron,  $P_{\pm}$ , which are defined as  $P_{+(-)} = \int_{z>(<)0} dz \int dR |\Psi(z, R, t)|^2$ . These are shown as the black solid ( $P_-$ ) and dashed ( $P_+$ ) lines in Fig. 1. It is evident from this figure that considerable electron localization occurs, with the electron density predominantly localized on the left (negative  $z$  axis).

We now propagate the electrons under the traditional potential Eq. (17), employing the exact TD mean nuclear position  $R(t)$  obtained from  $\Psi(z, R, t)$  by  $R(t) = \langle \Psi(z, R, t) | R | \Psi(z, R, t) \rangle$ , and calculate the electron localization probabilities, shown as red (or dark gray) solid line (negative region) and dashed line (positive region) in Fig. 1. Comparing the red (or dark gray) and black lines in Fig. 1, we find that the traditional potential yields the correct dynamics until around 5 fs, but then becomes less accurate: finally it predicts the electron to be almost perfectly localized on the left nucleus, while the exact calculation still gives some probability of finding the electron on the right.

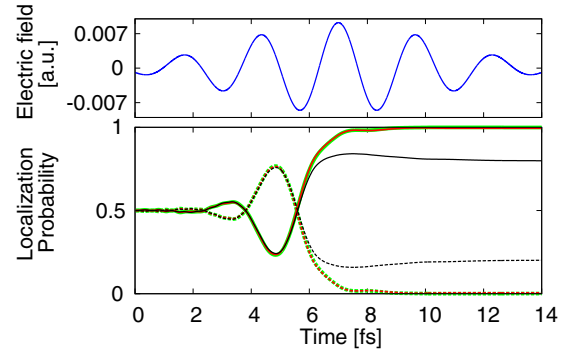


FIG. 1. (Color online) Electron localization probabilities along the negative (solid line) and the positive (dashed line)  $z$  axes as a function of time, obtained from exact dynamics (black), dynamics on the traditional potential  $\epsilon_e^{\text{trad}}$  evaluated at the exact mean nuclear position (red or dark gray), and dynamics on the approximate potential  $\epsilon_e^{\text{approx}}$  (green or light gray). The field is shown in the top panel.

To understand the error in the dynamics determined by the traditional surface, we compute the exact  $e$ -TD PES (12) in the gauge where the vector potential  $S(z, t)$  is zero [18]. In the upper panel of Fig. 2, the exact  $\epsilon_e$  [Eq. (12)] is plotted (black line) at three times [19], and compared with the traditional potential [Eq. (17)]  $\epsilon_e^{\text{trad}}$  (red or gray line) evaluated at the exact mean nuclear position. In the lower panel, the electron densities calculated from dynamics on the respective potentials are plotted.

A notable difference between  $\epsilon_e$  and  $\epsilon_e^{\text{trad}}$  is an additional interatomic barrier which appears in the exact potential, and a steplike feature that shifts one well with respect to the other. These additional features arise from the coupling terms contained in  $\Delta\epsilon$ , and are responsible for the correct dynamics, which is evident from the green (or light gray) curve in Fig. 1: this shows the results predicted by propagating the electrons on  $\epsilon_e^{\text{approx}}$ . The result is close to that of the red (or dark gray) traditional curve, and the potentials (not shown for figure clarity) are also close to the red (or gray) potentials shown

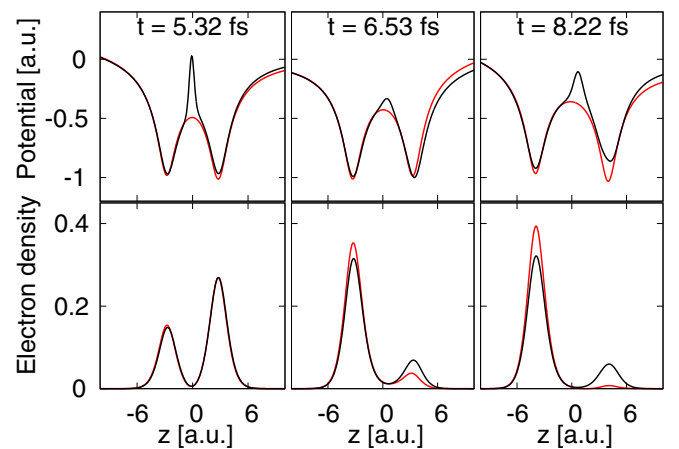


FIG. 2. (Color online) Top panel: Electronic potentials at the times indicated: exact  $\epsilon_e$  (black), and traditional  $\epsilon_e^{\text{trad}}$  evaluated at the exact mean nuclear position (red or gray). Lower panel: Electron densities obtained from dynamics on the electronic potentials shown at the indicated times in the top panel.

in Fig. 2. A TD Hartree treatment is also close to the results from propagating on  $\epsilon_e^{\text{trad}}$ . An examination of the different components in Eq. (16) shows that the additional interatomic barrier arises from the term  $\frac{1}{2m} \langle \frac{\partial}{\partial z} \chi_z | \frac{\partial}{\partial z} \chi_z \rangle_R$ , while the first two terms in Eq. (16) yield the step.

The current understanding of the mechanism for electron localization is that as the molecule dissociates, there is a rising interatomic barrier from  $W_{en}$ , which, when it reaches the energy level of the excited electronic state largely shuts off electron transfer between the ions [12]. The electron distribution is almost frozen after this point, as the electron can only tunnel between the nuclei. The additional barrier we see in the exact  $e$ -TDPES leads to an earlier localization time and ultimately smaller localization asymmetry. However, each of the three terms in Eq. (16) for  $\Delta\epsilon$  plays an important role in the dynamics: if the electronic system is evolved adding only the barrier correction to  $\epsilon_e^{\text{approx}}$  the localization asymmetry is somewhat reduced compared to evolving on  $\epsilon_e^{\text{approx}}$  alone, but far more so when all three terms of  $\Delta\epsilon$  are included.

In conclusion, we have shown that it is possible to describe the electronic subsystem coupled to nuclei and external fields via a TDSE, and given the exact form of the potentials appearing in this equation. The complete molecular wave function is factorized into electronic and nuclear wave functions  $\Psi(\underline{\mathbf{r}}, \underline{\mathbf{R}}, t) = \chi_e(\underline{\mathbf{R}}, t) \Phi(\underline{\mathbf{r}}, t)$ , where the electronic wave function  $\Phi(\underline{\mathbf{r}}, t)$  satisfies an electronic TDSE, and the nuclear wave function is conditionally dependent on the electronic coordinates. This is complementary to the factorization of Refs. [13,14,20],  $\Psi(\underline{\mathbf{r}}, \underline{\mathbf{R}}, t) = \chi(\underline{\mathbf{R}}, t) \Phi_{\mathbf{R}}(\underline{\mathbf{r}}, t)$ , where instead the nuclear wave function satisfies a TDSE while the electronic wave function does not. The exact  $e$ -TDPES and exact TD vector potential acting on the electrons were uniquely defined

and compared with the traditional potentials used in studying localization dynamics in a model of the  $\text{H}_2^+$  molecular ion. The importance of the exact  $e$ - $n$  correlation in the  $e$ -TDPES in reproducing the correct electron dynamics was demonstrated. Further studies on this and other model systems will lead to insight into how  $e$ - $n$  correlation affects electron dynamics in nonadiabatic processes, an insight that can never be gained from the classical electrostatic potentials caused by the point charges of the clamped nucleus nor the charge distributions of the exact nuclear density. Preliminary studies using the Shin-Metiu model [21] of field-free electronic dynamics in the presence of strong nonadiabatic couplings show that peak and shift structures in the exact  $e$ -TDPES, similar to those in the localization problem discussed here, appear typically after nonadiabatic transitions. Finally, we expect that the insight gained from the formalism and its analysis will lead to the derivation of approximate  $e$ - $n$  coupling potentials to be used in the development of practical and accurate electronic dynamics simulations. The exact TD electronic potentials defined in this study, together with the exact TD nuclear potentials derived in [13,14], establish the exact potential functionals of TD multicomponent density functional theory [17,22]. The study of these potentials may ultimately lead to approximate density functionals for use in this theory, which holds promise for the description of real-time coupled  $e$ - $n$  dynamics in real systems.

Partial support from the Deutsche Forschungsgemeinschaft (SFB 762), the European Commission (Grant No. FP7-NMP-CRONOS), and the US Department of Energy, Office of Basic Energy Sciences, Division of Chemical Sciences, Geosciences and Biosciences under Award No. DE-SC0008623 (N.T.M.), is gratefully acknowledged.

- 
- [1] G. Stefanucci and R. van Leeuwen, *Nonequilibrium Many Body Theory of Quantum Systems: A Modern Introduction* (Cambridge University Press, Cambridge, 2013); C. Attaccalite, M. Grüning, and A. Marini, *Phys. Rev. B* **84**, 245110 (2011).
  - [2] E. Runge and E. K. U. Gross, *Phys. Rev. Lett.* **52**, 997 (1984); C. A. Ullrich, *Time-Dependent Density-Functional Theory: Concepts and Applications* (Oxford University Press, Oxford, 2012); R. Baer, T. Seideman, S. Ilani, and D. Neuhauser, *J. Chem. Phys.* **120**, 3387 (2004).
  - [3] J. S. Jin, X. Zheng, and Y. J. Yan, *J. Chem. Phys.* **128**, 234703 (2008); X. Zheng, G. H. Chen, Y. Mo, S. K. Koo, H. Tian, C. Y. Yam, and Y. J. Yan, *ibid.* **133**, 114101 (2010).
  - [4] J. Caillat, J. Zanghellini, M. Kitzler, O. Koch, W. Kreuzer, and A. Scrinzi, *Phys. Rev. A* **71**, 012712 (2005); T. Kato and H. Kono, *J. Chem. Phys.* **128**, 184102 (2008); E. Y. Wilner, H. Wang, G. Cohen, M. Thoss, and E. Rabani, *Phys. Rev. B* **88**, 045137 (2013); I. Burghardt, K. Giri, and G. A. Worth, *J. Chem. Phys.* **129**, 174104 (2008).
  - [5] C. A. Rozzi *et al.*, *Nat. Commun.* **4**, 1602 (2013); W. R. Duncan and O. V. Prezhdo, *Annu. Rev. Phys. Chem.* **58**, 143 (2007).
  - [6] E. Tapavicza, I. Tavernelli, and U. Rothlisberger, *Phys. Rev. Lett.* **98**, 023001 (2007); D. Polli *et al.*, *Nature (London)* **467**, 440 (2010).
  - [7] E. Tapavicza, A. M. Meyer, and F. Furche, *Phys. Chem. Chem. Phys.* **13**, 20986 (2011).
  - [8] A. P. Horsfield, D. R. Bowler, A. J. Fisher, T. N. Todorov, and M. J. Montgomery, *J. Phys.: Condens. Matter* **16**, 3609 (2004); C. Verdozzi, G. Stefanucci, and C.-O. Almbladh, *Phys. Rev. Lett.* **97**, 046603 (2006); A. Nitzan and M. A. Ratner, *Science* **300**, 1384 (2003).
  - [9] T. Zuo and A. D. Bandrauk, *Phys. Rev. A* **52**, R2511 (1995); E. Räsänen and L. B. Madsen, *ibid.* **86**, 033426 (2012); J. Henkel, M. Lein, and V. Engel, *ibid.* **83**, 051401(R) (2011).
  - [10] S. Chelkowski, T. Zuo, O. Atabek, and A. D. Bandrauk, *Phys. Rev. A* **52**, 2977 (1995).
  - [11] J. C. Tully, *Faraday Discuss.* **110**, 407 (1998).
  - [12] G. Sansone *et al.*, *Nature (London)* **465**, 763 (2010); F. He, C. Ruiz, and A. Becker, *Phys. Rev. Lett.* **99**, 083002 (2007); F. Kelkensberg, G. Sansone, M. Y. Ivanov, and M. Vrakking, *Phys. Chem. Chem. Phys.* **13**, 8647 (2011).
  - [13] A. Abedi, N. T. Maitra, and E. K. U. Gross, *Phys. Rev. Lett.* **105**, 123002 (2010).
  - [14] A. Abedi, N. T. Maitra, and E. K. U. Gross, *J. Chem. Phys.* **137**, 22A530 (2012).
  - [15] E. Rabani and R. D. Levine, *J. Chem. Phys.* **104**, 1937 (1996).
  - [16] In this model system the electronic wave function  $\Phi(z, t)$  and density  $|\Phi(z, t)|^2$  are defined with respect to a coordinate frame

attached to the nuclear framework so that they are characteristic for the internal properties of the system [17].

- [17] T. Kreibich, R. van Leeuwen, and E. K. U. Gross, *Phys. Rev. A* **78**, 022501 (2008); T. Kreibich and E. K. U. Gross, *Phys. Rev. Lett.* **86**, 2984 (2001).
- [18] In general, both the scalar  $e$ -TDPES (12) and the vector potential (13) are present. In our specific one-dimensional example it is easy to see that the vector potential can be gauged away so that the  $e$ -TDPES remains as the only potential acting on the electronic subsystem [14]. This gauge is particularly useful for the comparison with traditional methods, because in those there is only a scalar potential acting on the electrons, allowing for a more direct comparison with the exact  $e$ -TDPES.
- [19] In Fig. 2, curves representing  $\epsilon_e$  have been rigidly shifted along the energy axis to compare with the traditional potentials.
- [20] A. Abedi, F. Agostini, Y. Suzuki, and E. K. U. Gross, *Phys. Rev. Lett.* **110**, 263001 (2013).
- [21] S. Shin and H. Metiu, *J. Chem. Phys.* **102**, 9285 (1995).
- [22] T.-C. Li and P.-Q. Tong, *Phys. Rev. A* **34**, 529 (1986).